Dalton Transactions

ROYAL SOCIETY OF CHEMISTRY

PAPER

View Article Online
View Journal | View Issue

Cite this: *Dalton Trans.*, 2022, **51**, 7241

Exploring the reactivity of homoleptic organozincs towards SO_2: synthesis and structure of a homologous series of organozinc sulfinates†

Adam Tulewicz, *[a] Vadim Szejko, [b] Iwona Justyniak, [a] Małgorzata Wolska-Pietkiewicz [b] and Janusz Lewiński *[a,b]

Studies on the reactivity of zinc alkyl compounds towards SO_2 are relatively less explored than either oxygenation or hydrolysis reactions. We report on the environmentally friendly and efficient syntheses of a homologous series of $[(RSO_2)ZnR]_n$ complexes from reactions involving homoleptic R_2Zn (R = Me, *t*Bu, Ph) compounds and SO_2. Diffusion ordered spectroscopy experiments indicate that the resulting compounds predominately occur as solvated dimers, $[(RSO_2)ZnR(THF)]_2$, in THF solution irrespective of the character of the group bonded to the zinc centres. In turn, these organozinc sulfinates exhibit structurally diversified molecular and supramolecular arrangements in the solid state, as evidenced by single-crystal X-ray diffraction studies. The methyl compound crystallises as a one-dimensional polymer, $[(MeSO_2)ZnMe]_n$, and the use of tBu_2Zn and Ph_2Zn leads to molecular aggregates, a tetramer $[(tBuSO_2)ZntBu]_4$, and a solvated $[(PhSO_2)ZnPh]_2{\cdot}2THF$ dimer, respectively. In addition, new theoretical insights have been gained by modelling the direct trapping of homoleptic organozinc compounds with SO_2 using DFT calculations.

Received 23rd February 2022,
Accepted 11th April 2022

DOI: 10.1039/d2dt00577h

rsc.li/dalton

Introduction

Studies on the reactivities of zinc alkyl compounds towards small inorganic molecules lie at the heart of organometallic chemistry. Primary attempts to react homoleptic organozinc compounds with small inorganic reagents can be traced back to the middle of the XIXth century.[1,2] Armoured with experimental creativity, it was Edward Frankland who synthesised 'zincethyl', known nowadays as diethylzinc, and reacted it with molecular dioxygen and water. The legacy of Frankland has continued ever since. Modern experiments performed in our group on the activation of dioxygen on Zn–C reactive species led to the isolation of the first alkylzinc alkylperoxides and provided a new look at the reactivities of zinc alkyls towards dioxygen.[3,4] Strikingly, the first structurally well-defined product derived from the hydrolysis of a dialkylzinc compound was reported only in 2011.[5] Since then, a set of compelling results regarding the hydrolysis of homo- and heteroleptic zinc alkyls including stable zinc hydroxide and zincoxane molecular clusters[6,7] or even ZnO quantum dots have been reported.[8–11] Furthermore, it was demonstrated that reactions between selected alkylzinc hydroxides and carbon dioxide could efficiently provide novel clusters and nanomaterials based on zinc carbonates with unique physicochemical properties.[12–14] In turn, studies on the reactivities of homoleptic and heteroleptic organozinc compounds towards SO_2 have been explored to a lesser extent, which may seem surprising, for example, in view of the potential use of heteroleptic zinc sulfinates as catalysts for the copolymerisation of CO_2 with epoxides[15–18] or zinc bis(alkanesulfinate)s as general reagents for the formation of radical species in organic synthesis.[19–22] The latter have been usually generated from the corresponding sulfonyl chlorides by treatment with zinc dust, and the requirement of a large excess of Zn metal has restricted their employment under *in situ* conditions.[19] Thus, the development of efficient synthetic procedures for zinc organosufinates is highly desirable.

To provide sufficient breadth and depth of literature coverage on the direct trapping of organometallic compounds with SO_2, we note that the research in the field started many decades ago and represents efficient methods for the preparation of a vast array of metal sulfinates,[19,23–28] featuring exceptionally rich coordination chemistry.[29–32] The renewed interest

[a]*Institute of Physical Chemistry, Polish Academy of Sciences, Kasprzaka 44/52, 01-224 Warsaw, Poland. E-mail: atulewicz@ichf.edu.pl, lewin@ch.pw.edu.pl*
[b]*Department of Chemistry, Warsaw University of Technology, Noakowskiego 3, 00-664 Warsaw, Poland*

†Electronic supplementary information (ESI) available: Synthetic procedures, spectroscopic and crystallographic data, and computation details. CCDC 2116783–2116785. For ESI and crystallographic data in CIF or other electronic format see DOI: **https://doi.org/10.1039/d2dt00577h**

has been rekindled by reactions of frustrated Lewis pairs or related compounds with SO_2.[32–37] Remarkably, to our knowledge, there are only two reports where the crystal structures of the products of SO_2 insertion into homoleptic organozincs have been investigated. Roesky *et al.*[38] showed that the reaction between SO_2 and zincocens affords a double insertion product, $[Zn(O_2SCp^*)_2(tmeda)]$, as well as $[Zn_4(O_2SCp^*)_6O]$ clusters that contain a Zn_4O structural motif. Moreover, thermal decomposition of $[Zn(O_2SCp^*)_2(tmeda)]$ resulted in the formation of $[Zn_2(\mu\text{-}SO_3)(\mu\text{-}S_2O_4)(tmeda)_2]$. The latter result carries valuable information on the thermodynamic stability of the O_2SCp^{*-} anion, in particular, regarding the possibility of its transformations into other ions, *i.e.*, sulfuroxo anions. More recently, our group initiated studies on the Et_2Zn/SO_2 system.[39] We showed that various multidimensional networks bearing either $(EtSO_2)ZnEt$ or $(EtSO_2)_2Zn$ motifs could be obtained with respect to (i) the reaction stoichiometry, (ii) the presence of a certain Lewis base and (iii) the type of solvent chosen for performing the reaction.

We and others have well documented that the character of Zn-bonded alkyl groups dramatically affects the reactivity of organozincs towards small molecules and the composition and structure of the resulting products.[40–46] Driven by both curiosity to explore new aspects of reactivities of organozinc systems towards SO_2 and the search for new (L)ZnR-type precursors or building blocks of functional materials, herein we turn our attention to the studies of equimolar reactions between selected homoleptic organozinc compounds with SO_2. In particular, we report on reactions between R_2Zn (R = Me, *t*Bu, Ph) and SO_2 in THF, which allowed for the synthesis of a homologous series of organozinc sulfinates in the form of solvated $[(RSO_2)ZnR(THF)]_2$ dimers in a THF solution, and the isolation of structurally diversified molecular and supramolecular arrangements in the solid state, *i.e.*, a one-dimensional coordination polymer $[(MeSO_2)ZnMe]_n$ (**1**), a tetrameric cluster $[(tBuSO_2)ZntBu]_4$ (**2**) to a solvated dimer of the formula $[(PhSO_2)ZnPh]_2{\cdot}2THF$ (**3**), respectively (Scheme 1).

Results and discussion

Synthesis and spectroscopic characterisation

Immediate reactions between R_2Zn (R = Me, *t*Bu, Ph) and gaseous SO_2 in the molar ratio 1 : 1 were carried out according to Scheme 1. Colourless cubic crystals of either **1**, **2** or **3** were isolated in high yield after standard workup (for details, see the Experimental section). Compounds **1–3** were fully characterised using elemental analysis, spectroscopic and single-crystal X-ray diffraction techniques. The FTIR spectra of compounds **1–3** comprise intense to medium bands in the range 876–1043 cm^{-1}, assigned to the sulfur–oxygen vibrations,[35] which confirms the presence of the sulfinate anion. The ^1H NMR spectrum of **1** shows two well-resolved singlets at 2.38 ppm and −0.91 ppm, derived from the protons of $MeSO_2$ and MeZn groups, respectively (see the ESI, Fig. S1†), while the ^{13}C NMR spectrum of **1** shows two signals at 49.33 ppm and −16.9 ppm from the carbon atoms of the methylsulfinate anion and the Zn-Me group, respectively (see the ESI, Fig. S2†). Similarly, inspection of the ^1H NMR spectrum of **2** reveals two separated sharp singlets at 1.07 ppm and 1.01 ppm with equal intensities, assigned to the methyl protons of $tBuSO_2$ and *t*BuZn groups, respectively (see the ESI, Fig. S4†). The ^{13}C NMR spectrum of **2** shows two intensive sharp singlets of the primary carbons of the $tBuSO_2$ and *t*BuZn groups at 32.89 ppm and 20.77 ppm, respectively. Less intensive signals from the quaternary carbons were found at 55.42 ppm and 19.72 ppm, respectively (see the ESI, Fig. S5†). The ^1H NMR spectrum of **3** comprises an overlapping multiplet from phenyl protons that fall within a range between 6.98 ppm and 7.79 ppm. In addition, the characteristic multiplets of THF protons were

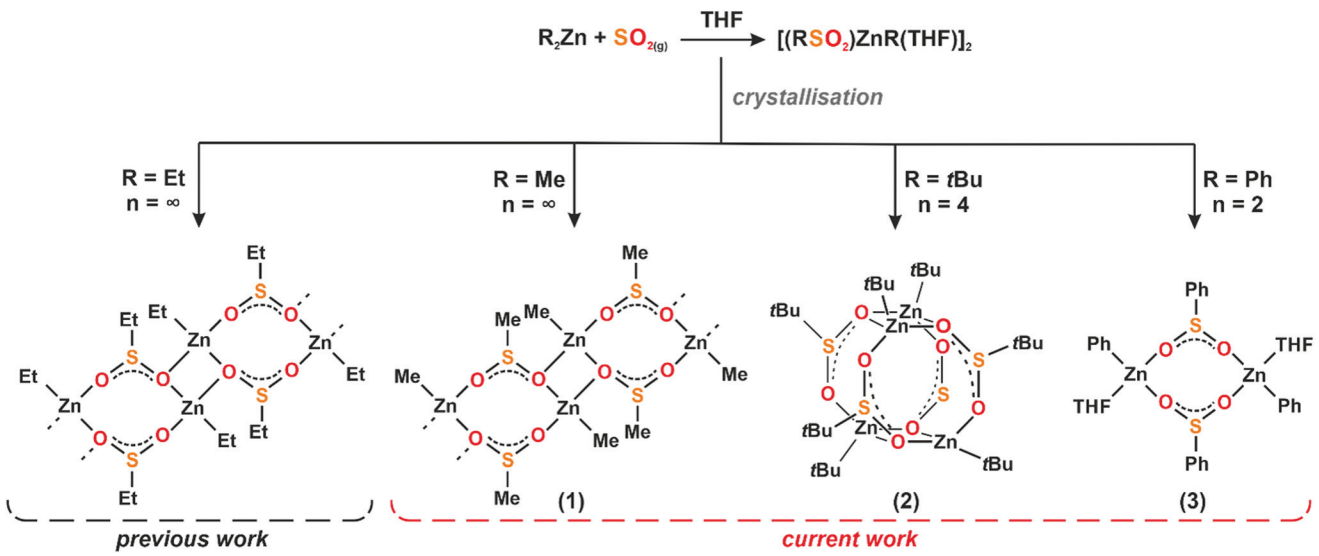

Scheme 1 Reactivity of Me_2Zn, tBu_2Zn and Ph_2Zn towards SO_2 leading to $(MeSO_2)ZnMe$ (**1**), $(tBuSO_2)ZntBu$ (**2**) and $(PhSO_2)ZnPh$ (**3**).

recorded at 1.77 ppm and 3.62 ppm, with the intensities indicative of the partial desolvation of compound **3** (see the ESI, Fig. S7†). The ^{13}C NMR spectrum of **3** features signals from the phenyl groups at 153.11 and 152.38 ppm, and in the range of 139.59–125.62 ppm. Signals assigned to the secondary and primary carbons of THF were found at 26.37 ppm and 68.25 ppm, respectively. Moreover, the DOSY experiments indicate that compounds **1–3** occur as solvated dimers $[(RSO_2)ZnR(THF\text{-}d_8)]_2$ in THF-d_8 solution irrespective of the character of the alkyl group bonded to zinc centres (for details, see the ESI†).

Furthermore, some combinations of heteroleptic (L)ZnR-type complexes with homoleptic R_2Zn compounds act as arguably the most important organozinc catalytic systems in organic synthesis[47,48] or precursors of various functional materials.[14,49] Nevertheless, the chemistry of (L)ZnR/R_2Zn systems remains both relatively poorly understood and a subject of constant debate.[50,51] Thus, we performed controlled experiments on the reactivity of selected $[(RSO_2)ZnR]/R'_2Zn$ systems. In this regard, we prepared THF solutions of **1** and **2** that were subsequently treated with equimolar amounts of tBu$_2$Zn and Me$_2$Zn, respectively (Scheme 2). Strikingly, we found that in the first case, $(MeSO_2)ZnMe/t Bu_2Zn$, the zinc-bonded methyl group was easily substituted by the *tert*-butyl group (see the ESI, Fig. S10 and 11†). Conversely, in the case of the $(t BuSO_2)Znt Bu/Me_2Zn$ system no exchange was observed as indicated by the NMR studies (see the ESI, Fig. S12 and 13†). The reasons for such different reactivities are unclear and must be further investigated.

Solid-state structures

Remarkably, the nature of the zinc-bonded alkyl substituents has a profound effect on the solid-state structure of the title organozinc sulfinates. Compound **1** crystallises in triclinic space group $P\bar{1}$ as a 1D coordination polymer constructed of dinuclear $[(MeSO_2)ZnMe]_2$ units incorporating sulfinato-O,O′-type ligands (Fig. 1) and interconnected through the $[Zn_2(\mu_2\text{-}O_2)]$ rings to form an extended chain along the *a* axis. The structural constitution of **1** reflects the polymeric structure of the previously reported ethylzinc ethylsulfinate derivative,[38] $[(EtSO_2)ZnEt]_n$. The Zn–O bond distances within the molecular $[(MeSO_2)ZnMe]_2$ unit fall in the range of 1.988–2.096 Å, and the Zn–O bonds connecting these units are of a similar length of 2.075 Å. The S–C bond length is 1.772 Å, and the S–O bonds of length 1.517–1.551 Å, along with O–S–O angles (106.9°), are similar to values observed for other metal sulfinate complexes.[30,38,39]

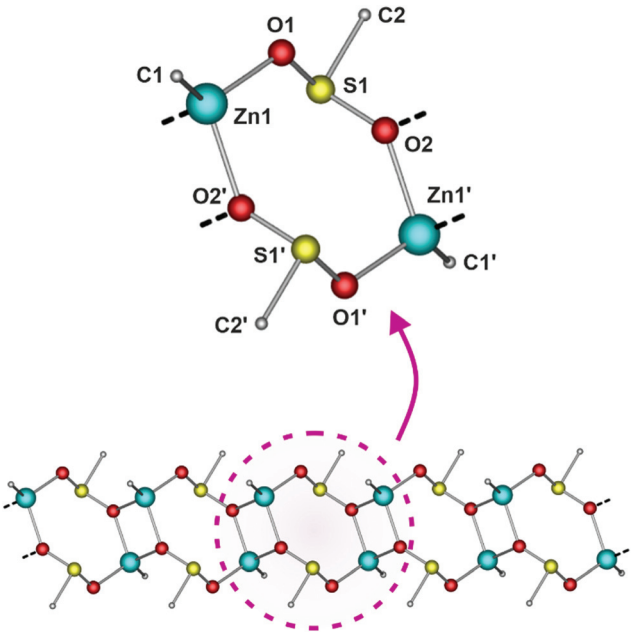

Fig. 1 Molecular structure and single polymeric chain (view along the crystallographic *a* axis) of **1**. Hydrogen atoms have been omitted for clarity.

Compound **2** crystallises in the $P\bar{1}$ triclinic space group. An inspection of the structure of **2** revealed that metal centres adopt a tetrahedral geometry, and four tBuZn moieties are stabilised by four *tert*-butylsulfinate anions (Fig. 2a). As a result, the molecular structure of **2** comprises two sulfinato-O, O′-type $[(t BuSO_2)Znt Bu]_2$ heterocycles joined within two $[Zn_2(\mu_2\text{-}O_2)]$ moieties forming tetranuclear cluster $[(t BuSO_2)Znt Bu]_4$. Interestingly, the core of compound **2** is isostructural to quasi-cube-shaped *tert*-buthylzinc diorganophosphate $[t BuZn(O_2P(OR)_2)]$ (R = Me, Ph) complexes previously reported by us.[52] The Zn–O bond lengths in **2** were found to be in the range between 2.005 and 2.121 Å and the S–O distances between 1.510 and 1.555 Å, similar to the bond values found in the case of compound **1** and related alkylzinc sulfinates.[39] Compound **3** crystallises in triclinic space group $P\bar{1}$. An introduction of the aromatic group provided dinuclear solvate $[(PhSO_2)ZnPh(THF)]_2$ (Fig. 2b). Two metal centres of **3** are connected by the $PhSO_2$-μ_2-bridging moieties forming an octanuclear macrocycle that adopts a chair conformation similar to that observed for compound **1**, with the phenyl groups located *trans* to each other across the ring. However, contrary to **1** and **2**, the tetrahedral coordination sphere located on each metal centre of **3** is completed by a single THF molecule. That results in a monomeric structural motif, preferable over either the 1D coordination polymer or tetranuclear cluster, likely due to the steric hindering introduced by phenyl rings. The Zn–$O_{sulfinate}$ distances of **3** are observed to be in the range of 1.987–2.088 Å, and the Zn–O_{THF} bonds to outer solvent molecules are longer

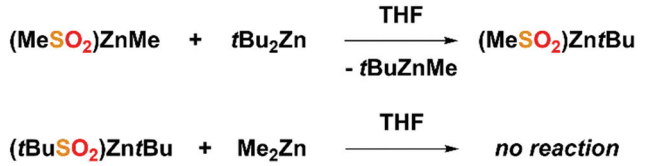

Scheme 2 Controlled experiments on the reactivities of $[(RSO_2)ZnR]$ species towards homoleptic organozincs.

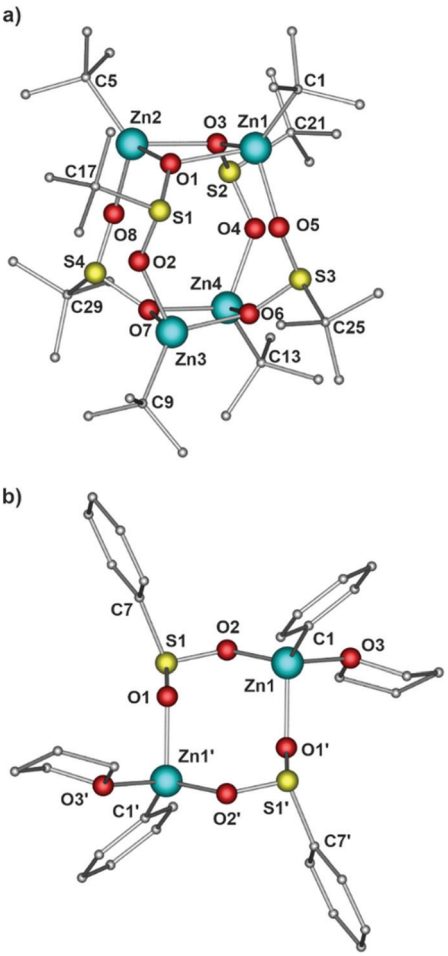

Fig. 2 Molecular structure of **2** (a) and **3** (b). Hydrogen atoms have been omitted for clarity.

and are of length 2.088 Å. The S–O bonds are similar within the molecule and their lengths are between 1.527 and 1.528 Å. The O–S–O conical angles (107.37°) together with the aforementioned parameters are similar to that observed for other zinc sulfinate compounds.[30,38,39]

DFT studies

DFT calculations were subsequently performed to explore the thermodynamic landscape associated with insertions of SO_2 into the studied systems as well as to deeply investigate the studies on the reactivity of SO_2 towards various alkylzincs (Fig. 3). In all the considered cases, the reaction between R_2Zn and SO_2 starts with the formation of van der Waals complexes, where the oxygen atom from SO_2 is attracted by the metal centre, similarly to our previous studies with Et_2Zn/SO_2 systems. In the next step, the formation of the transition state occurs. In the case of Ph_2Zn/SO_2, the geometry of the transition state remains only slightly distorted, in contrast to the geometries of transition states found within the Me_2Zn/SO_2 and tBu$_2$Zn/SO_2 systems. This may explain to some extent the relatively low barrier of reaction found for the insertion of SO_2 into Ph_2Zn. Note that the elongation of the Zn–C bond, associated with the R_2Zn/SO_2 transition state, is energetically highly unfavoured, in particular for the small alkyls. This effect may explain the higher value of the energy barrier of +14.9 kcal mol^{-1}, found for the insertion of SO_2 into Me_2Zn. Finally, the overall energetic effect of the R_2Zn/SO_2 reactions remains highly negative and similar to the results obtained within related studies,[24,25] and suggests that reactions between R_2Zn and SO_2 should be driven in a one way direction.

Experimental section

General remarks

All reactions and post-synthetic manipulations were conducted under an argon or nitrogen atmosphere using standard Schlenk and glovebox techniques (MBraun UniLab Plus; <0.1 ppm O_2, <0.1 ppm H_2O). All solvents were purified by passage through activated aluminium oxide (MBraun SPS) and stored over 3 Å molecular sieves. Prior to use, deuterated solvents were dried over Na/K, distilled under an argon atmosphere before use, and stored over molecular sieves. Di-*tert*-butylzinc was prepared according to the literature procedure.[53] All reagents used in this study were of commercial grade and

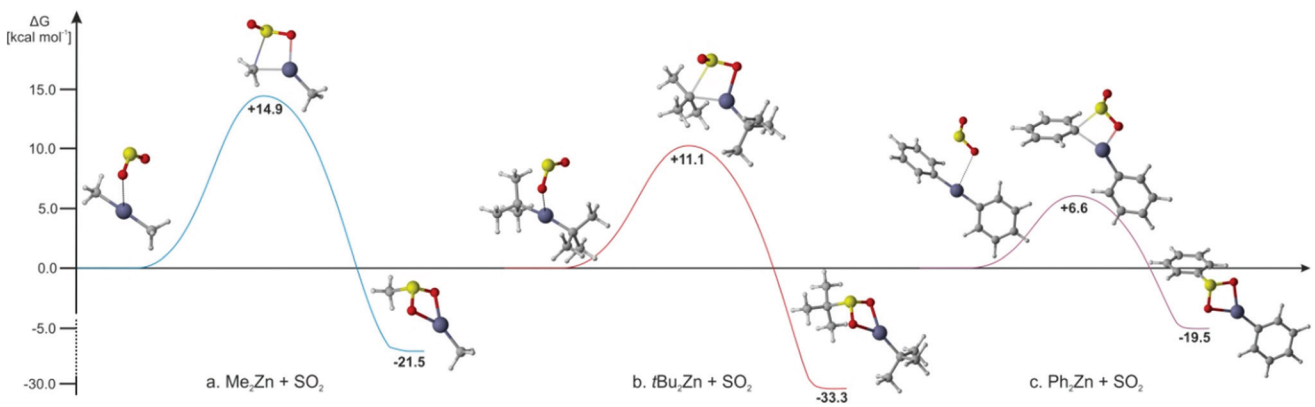

Fig. 3 The comparison of reaction pathways of SO_2 insertion into Me_2Zn (a; blue line), tBu$_2$Zn (b; red line) and Ph_2Zn (c; violet line). The values of ΔG have been referenced to the Gibbs free energies of the van der Waals complexes.

obtained from Sigma-Aldrich Co or abcr GmbH. Stoichiometric amounts of SO_2 (determined by using the Clausius–Clapeyron equation) were added to the reaction mixtures through a syringe. NMR spectra were acquired with a Varian Mercury 400 MHz spectrometer at 298 K unless otherwise specified and were referenced to the residual ^1H or ^{13}C signals of the deuterated solvents. FTIR spectra were recorded with a Bruker Vertex 80V spectrometer equipped with a diamond ATR (attenuated total reflection) unit. Elemental analysis was performed by using a UNICUBE (Elementar Analysensysteme GmbH).

Synthesis of $[(MeSO_2)ZnMe]_n$ (1). To Me_2Zn (0.35 mL of *ca.* 2 M solution in hexane, 0.7 mmol) was added THF (5 mL) and then 1 equiv. of SO_2 (*ca.* 17.1 cm^3, 298 K, 1 atm) was condensed onto the stirring solution at room temperature. The reaction mixture was then stirred for an additional 1 h. The solution was then dried under vacuum and the solid residue, obtained after the removal of the solvent, was afterwards dissolved in THF (1 mL). Compound **1** was obtained as colourless, long needle-shaped crystals after crystallisation at RT. Isolated yield: 98 mg, 88%; ^1H NMR (400 MHz, THF-d_8, 298 K) δ = 2.38 (s, 3H; CH_3SO_2), −0.91 (s, 3H; CH_3Zn) ppm. ^{13}C NMR (101 MHz, THF-d_8, 298 K) δ = 49.33 ppm. IR (ATR): 2951 (vw), 2906 (vw), 2843 (vw), 1415 (vw), 1397 (vw), 1302 (vw), 1155 (vw), 1004 (s), 958 (s), 945 (s), 895 (vs), 703 (w), 674 (m), 538 (s), 450 (w) cm^{-1}. Elemental analysis calcd (%) for $C_4H_{12}O_4S_2Zn_2$ (319.02): C 15.06, H 3.79, S 20.10; found (%): C 14.96, H 3.63, S 18.54.

Synthesis of $[(tBuSO_2)ZntBu]_4$ (2). The procedure was similar to that described for **1**, but was carried out by using *ca.* 0.8 M solution of tBu_2Zn in toluene. Compound **2** was obtained as colourless, long needle-shaped crystals after crystallisation at RT. Isolated yield: 158 mg, 93%; ^1H NMR (400 MHz, THF-d_8, 298 K) δ = 1.07 (s, 9H; $(CH_3)_3CSO_2$), 1.01 (s, 9H; $(CH_3)_3CZn$) ppm. ^{13}C NMR (101 MHz, THF-d_8, 298 K) δ = 55.42, 32.89, 20.77, 19.72 ppm. IR (ATR): 2978 (vw), 2940 (vw), 2918 (vw), 2862 (vw), 2808 (w), 2755 (vw), 2695 (vw), 1473, (vw), 1461 (w), 1388 (vw), 1360 (w), 1187 (vw), 1043 (s), 1007 (m), 967 (m), 889 (vs), 815 (w), 790 (w), 689 (vw), 613 (s), 552 (w), 516 (vw), 463 (vw), 437 (w) cm^{-1}. Elemental analysis calcd (%) for $C_{32}H_{72}O_8S_4Zn_4$ (974.68): C 39.43, H 7.45, S 13.16; found (%): C 39.67, H 7.12, S 12.82.

Synthesis of $[(PhSO_2)ZnPh]_2$ (3). The procedure was similar to that described for **1**, but was carried out by using 0.153 g (0.7 mmol) of Ph_2Zn. Compound **3** was obtained as colourless, long needle-shaped crystals after crystallisation from a THF solution at −20 °C. Isolated yield: 150 mg, 76%; ^1H NMR (400 MHz, THF-d_8, 298 K) δ = 7.79–7.73 (m, 2H, C–H_{Ar}), 7.46–7.37 (m, 5H, C–H_{Ar}), 7.06–6.98 (m, 3H, C–H_{Ar}), 3.65–3.59 (m, 2H, –OCH_2^{THF}–), 1.80–1.74 (m, 2H, –CH_2^{THF}–) ppm. ^{13}C NMR (101 MHz, THF-d_8, 298 K) δ = 153.11, 152.38, 139.59, 131.30, 129.41, 127.22, 126.32, 125.62, 68.25, 26.37 ppm. IR (ATR): 3060 (vw), 3030 (vw), 2981 (vw), 2889 (vw), 1583 (vw), 1475 (w), 1442 (w), 1419 (w), 1249 (vw), 1177 (vw), 1088 (w), 1003 (s), 990 (s), 954 (vs), 876 (m), 754 (s), 722 (w), 702 (s), 685 (s), 584 (m), 502 (w), 473 (m), 443 (m) cm^{-1}. Elemental analysis calcd (%) for $C_{32}H_{36}O_6S_2Zn_2$ (711.51): C 54.02, H 5.10, S 9.01; found (%): C 53.69, H 4.64, S 8.46.

Reaction of 1 with tBu_2Zn. To the THF solution of $[(MeSO_2)ZnMe]$ (0.8 mmol) obtained in the aforementioned procedure was added tBu_2Zn (1 ml of *ca.* 0.8 M solution in toluene, 0.8 mmol). The reaction mixture was then stirred for 1 h. After the standard workup the solid residue was subjected to NMR studies.

Reaction of 2 with Me_2Zn. The procedure was similar to that described for the reaction between **1** and tBu_2Zn carried out by using (0.7 mmol) $[(tBuSO_2)ZntBu]$ and Me_2Zn (0.35 mL of *ca.* 2 M solution in hexane, 0.7 mmol).

X-Ray structure determination

The X-ray data for complexes **1**, **2**, and **3** were collected at 100 (2) K on a SuperNova Agilent diffractometer using graphite monochromated MoKα radiation (λ = 0.71073 Å). The data were processed with CrysAlisPro.[54] The structure was solved by direct methods using the SHELXS-97 program and was refined by full matrix least-squares on F^2 using the program SHELXL.[55] All non-hydrogen atoms were refined with anisotropic displacement parameters. Hydrogen atoms were added to the structure model at geometrically idealised coordinates and refined as riding atoms.

Crystal data for 1 (CCDC-2116783†). $[C_2H_6O_2SZn]_n$: M = 159.50, triclinic, space group $P\bar{1}$ (no. 2), a = 4.5135(8) Å, b = 7.7984(11) Å, c = 7.8400(13) Å, α = 89.141(12)°, β = 80.887(14)°, γ = 84.090(13)°, U = 271.02(8) Å^3, Z = 2, F(000) = 160, D_c = 1.954 g cm^{-3}, μ(Mo-Kα) = 4.785 mm^{-1}, θ_{max} = 26.500°, 1117 unique reflections. Refinement converged at $R1$ = 0.0701, w$R2$ = 0.1688 for all data ($R1$ = 0.0632, w$R2$ = 0.1609 for 977 reflections with $I_o > 2\sigma(I_o)$). The goodness-of-fit on F^2 was equal to 1.088.

Crystal data for 2 (CCDC-2116784†). $C_{32}H_{72}O_8S_4Zn_4$: M = 974.61, triclinic, space group $P\bar{1}$ (no. 2), a = 11.9492(3) Å, b = 12.8183(7) Å, c = 16.1223(5) Å, α = 86.157(3)°, β = 78.812(2)°, γ = 75.515(3)°, U = 2345.05(16) Å^3, Z = 2, F(000) = 1024, D_c = 1.380 g cm^{-3}, μ(Mo-Kα) = 2.238 mm^{-1}, θ_{max} = 26.997°, 10 221 unique reflections. Refinement converged at $R1$ = 0.0611, w$R2$ = 0.0720 for all data ($R1$ = 0.0374, w$R2$ = 0.0646 for 7731 reflections with $I_o > 2\sigma(I_o)$). The goodness-of-fit on F^2 was equal to 1.019.

Crystal data for 3 (CCDC-2116785†). $C_{32}H_{36}O_6S_2Zn_2$: M = 711.47, triclinic, space group $P\bar{1}$ (no. 2), a = 8.792(5) Å, b = 9.326(5) Å, c = 10.669(5) Å, α = 78.722(5)°, β = 74.655(5)° γ = 67.772(5)°, U = 776.4(7) Å^3, Z = 1, F(000) = 368, D_c = 1.522 g cm^{-3}, μ(Mo-Kα) = 1.722 mm^{-1}, θ_{max} = 30.163°, 3931 unique reflections. Refinement converged at $R1$ = 0.0449, w$R2$ = 0.0872 for all data ($R1$ = 0.0361, w$R2$ = 0.0826 for 3412 reflections with $I_o > 2\sigma(I_o)$). The goodness-of-fit on F^2 was equal to 1.050.

Theoretical details

The geometries of the molecules chosen as model systems were optimised by using density functional theory (DFT) with the B3LYP[56,57] functional in the 6-31++G(2d,2p) basis set with the D3(BJ) correction[58,59] added in order to improve the

description of dispersion forces. Frequency analysis was performed in order to confirm the nature of minima and maxima. Intrinsic reaction coordinate calculations (IRC)[60] were additionally done to check the quality of the transition states. All the calculations were done with the Gaussian suite of codes.[61] Figures have been prepared with the CYLview visualisation software.[62]

Conclusions

Finding new potential (L)ZnR-type reagents for organic synthesis or precursors of nanomaterials that can be efficiently synthesised from some air pollutants may represent an important step toward a better future. Simultaneously, explorations of reactivity of homoleptic dialkylzincs towards sulfur dioxide still leave many opportunities for scientific discoveries. In this vein, we performed the first systematic studies on the effect of the nature of Zn-bonded alkyl groups on both the SO_2 insertion process and structure of the resulting products in the solid state and solution. The direct trapping of homoleptic R_2Zn compounds with SO_2 allowed for the isolation and characterisation of a homologous series of organozinc sulfinate [$(RSO_2)ZnR$] species that are hardly accessible with alternative methods. Moreover, we showed that the resulting organozinc sulfinates occur as solvated dimers $[(RSO_2)ZnR(THF)]_2$ in THF solution irrespective of the character of the substituent. In turn, the identity of the Zn-R group determines whether the $[(RSO_2)ZnR]_n$ product acquires a dimeric, tetrameric or 1D-polymeric constitution in the solid state. Interestingly, the DFT calculations performed on the set of equimolar R_2Zn/SO_2 systems confirm that the SO_2 insertion into the Zn–C bond can be characterised by a moderate value of the energy barriers and the highly exothermic character of the SO_2 insertion.

Finally, the reported investigations fill a missing gap in the realm of (L)ZnR complexes as new precursors of functional materials and further studies on the application of organozinc sulfinates as efficient precursors of surface-modified ZnO nanostructures are in progress.

Conflicts of interest

There are no conflicts to declare.

Acknowledgements

The authors gratefully acknowledge the National Science Centre, Poland (grant OPUS 2017/25/B/ST5/02484 and grant MINIATURA 2021/05/X/ST4/00520) for financial support. Moreover, the ICM University of Warsaw Computer Center is acknowledged for facilities and computer time allocation within the grant G70-21. The authors would also like to thank Dr Piotr Bernatowicz for assistance with DOSY experiments.

Notes and references

1 E. von Frankland, *Justus Liebigs Ann. Chem.*, 1849, **71**, 171–213.
2 D. Seyferth, *Organometallics*, 2001, **20**, 2940–2955.
3 J. Lewiński, W. Śliwiński, M. Dranka, I. Justyniak and J. Lipkowski, *Angew. Chem., Int. Ed.*, 2006, **45**, 4826–4829.
4 T. Pietrzak, I. Justyniak, M. Kubisiak, E. Bojarski and J. Lewiński, *Angew. Chem., Int. Ed.*, 2019, **58**, 8526–8530.
5 W. Bury, E. Krajewska, M. Dutkiewicz, K. Sokołowski, I. Justyniak, Z. Kaszkur, K. J. Kurzydłowski, T. Płociński and J. Lewiński, *Chem. Commun.*, 2011, **27**, 5467–5469.
6 D. Prochowicz, K. Sokołowski and J. Lewiński, *Coord. Chem. Rev.*, 2014, **270–271**, 112–126.
7 K. Sokołowski, I. Justyniak, W. Śliwiński, K. Sołtys, A. Tulewicz, A. Kornowicz, R. Moszyński, J. Lipkowski and J. Lewiński, *Chem. – Eur. J.*, 2012, **18**, 5637–5645.
8 D. Lee, M. Wolska-Pietkiewicz, S. Badoni, A. Grala, J. Lewiński and G. De Paëpe, *Angew. Chem., Int. Ed.*, 2019, **58**, 17163–17168.
9 M. Terlecki, S. Badoni, M. K. Leszczyński, S. Gierlotka, I. Justyniak, H. Okuno, M. Wolska-Pietkiewicz, D. Lee, G. De Paëpe and J. Lewiński, *Adv. Funct. Mater.*, 2021, 2105318.
10 Z. Zhao, Y. Wang, C. Delmas, C. Mingotaud, J. D. Marty and M. L. Kahn, *Nanoscale Adv.*, 2021, **3**, 6696–6703.
11 P. Krupiński, A. Grala, M. Wolska-Pietkiewicz, W. Danowski, I. Justyniak and J. Lewiński, *ACS Sustainable Chem. Eng.*, 2021, **9**, 1540–1549.
12 K. Sokołowski, W. Bury, I. Justyniak, D. Fairen-Jimenez, K. Sołtys, D. Prochowicz, S. Wang, M. Schröder and J. Lewiński, *Angew. Chem., Int. Ed.*, 2013, **52**, 13414–13418.
13 K. Sokołowski, W. Bury, I. Justyniak, A. M. Cieślak, M. Wolska, K. Sołtys, I. Dzięcielewski and J. Lewiński, *Chem. Commun.*, 2013, **49**, 5271.
14 K. Sokołowski, W. Bury, A. Tulewicz, A. M. Cieślak, I. Justyniak, D. Kubicki, E. Krajewska, A. Milet, R. Moszyński and J. Lewiński, *Chem. – Eur. J.*, 2015, **21**, 5496–5503.
15 R. Eberhardt, M. Allmendinger, M. Zintl, C. Troll, G. A. Luinstra and B. Rieger, *Macromol. Chem. Phys.*, 2004, **205**, 42–47.
16 B. Y. Lee, H. Y. Kwon, S. Y. Lee, S. J. Na, S. Han, H. Yun, H. Lee and Y. Park, *J. Am. Chem. Soc.*, 2005, **127**, 3031–3037.
17 M. F. Pilz, C. Limberg, B. B. Lazarov, K. C. Hultzsch and B. Ziemer, *Organometallics*, 2007, **26**, 3668–3676.
18 R. Eberhardt, M. Allmendinger, G. A. Luinstra and B. Rieger, *Organometallics*, 2008, **22**, 211–214.
19 F. O'Hara, R. D. Baxter, A. G. O'Brien, M. R. Collins, J. A. Dixon, Y. Fujiwara, Y. Ishihara and P. S. Baran, *Nat. Protoc.*, 2013, **8**, 1042–1047.
20 D. Kaiser, I. Klose, R. Oost, J. Neuhaus and N. Maulide, *Chem. Rev.*, 2019, **119**, 8701–8780.
21 S. Liang, K. Hofman, M. Friedrich and G. Manolikakes, *Eur. J. Org. Chem.*, 2020, 4664–4676.

22 J. L. Nova-Fernández, M. J. García, L. Mollari, G. Pascual-Coca, S. Cabrera and J. Alemán, *Chem. Commun.*, 2022, **58**, 4611–4614.
23 A. Wojcicki, *Acc. Chem. Res.*, 1971, **598**, 344–352.
24 A. Wojcicki, in *Advances in Organometallic Chemistry*, Elsevier, 1974, pp. 31–81.
25 R. G. Severson and A. Wojcicki, *J. Am. Chem. Soc.*, 1979, **5**, 877–883.
26 C. E. Kefalidis, C. Jones and L. Maron, *Dalton Trans.*, 2016, **45**, 14789–14800.
27 E. Louyriac, P. W. Roesky and L. Maron, *Dalton Trans.*, 2017, **46**, 7660–7663.
28 J. M. Smith, J. A. Dixon, J. N. Degruyter and P. S. Baran, *J. Med. Chem.*, 2019, **62**, 2256–2264.
29 W. A. Schenk, *Angew. Chem., Int. Ed. Engl.*, 1987, **26**, 98–109.
30 W. A. Schenk, *Dalton Trans.*, 2011, **40**, 1209–1219.
31 A. J. Boutland, I. Pernik, A. Stasch and C. Jones, *Chem. – Eur. J.*, 2015, **21**, 15749–15758.
32 S. V. Klementyeva, N. Arleth, K. Meyer, S. N. Konchenko and P. W. Roesky, *New J. Chem.*, 2015, **39**, 7589–7594.
33 M. Sajid, A. Klose, B. Birkmann, L. Liang, B. Schirmer, T. Wiegand, H. Eckert, A. J. Lough, R. Fröhlich, C. G. Daniliuc, S. Grimme, D. W. Stephan, G. Kehr and G. Erker, *Chem. Sci.*, 2013, **4**, 213–219.
34 D. W. Stephan and G. Erker, *Chem. Sci.*, 2014, **5**, 2625–2641.
35 K. Y. Ye, M. Bursch, Z. W. Qu, C. G. Daniliuc, S. Grimme, G. Kehr and G. Erker, *Chem. Commun.*, 2017, **53**, 633–635.
36 N. Aders, L. Keweloh, D. Pleschka, A. Hepp, M. Layh, F. Rogel and W. Uhl, *Organometallics*, 2019, **38**, 2839–2852.
37 N. Szynkiewicz, J. Chojnacki and R. Grubba, *Inorg. Chem.*, 2020, **59**, 6332–6337.
38 R. P. Kelly, N. Kazeminejad, C. A. Lamsfus, L. Maron and P. W. Roesky, *Chem. Commun.*, 2016, **52**, 13090–13093.
39 A. Tulewicz, M. Wolska-Pietkiewicz, M. Jędrzejewska, T. Ratajczyk, I. Justyniak and J. Lewiński, *Chem. – Eur. J.*, 2019, **25**, 14072–14080.
40 S. Jana, R. J. F. Berger, R. Fröhlich, T. Pape and N. W. Mitzel, *Inorg. Chem.*, 2007, **46**, 4293–4297.
41 I. Dranka, M. Kubisiak, I. Justyniak, M. Lesiuk, D. Kubicki and J. Lewiński, *Chem. – Eur. J.*, 2011, **17**, 12713–12721.
42 M. Kubisiak, K. Zelga, W. Bury, I. Justyniak, K. Budny-Godlewski, Z. Ochal and J. Lewiński, *Chem. Sci.*, 2015, **6**, 3102–3108.
43 T. Pietrzak, M. D. Korzyński, I. Justyniak, K. Zelga, A. Kornowicz, Z. Ochal and J. Lewiński, *Chem. – Eur. J.*, 2017, **23**, 7997–8005.
44 Z. Wrobiel, T. Pietrzak, I. Justyniak and J. Lewiński, *Chem. Commun.*, 2017, **53**, 10808–10811.
45 K. Budny-Godlewski, I. Justyniak, M. K. Leszczyński and J. Lewiński, *Chem. Sci.*, 2019, **10**, 7149–7155.
46 Ł. Mąkolski, V. Szejko, K. Zelga, A. Tulewicz, P. Bernatowicz, I. Justyniak and J. Lewiński, *Chem. – Eur. J.*, 2021, **27**, 5666–5674.
47 L. Pu and H. Yu, *Chem. Rev.*, 2001, **101**, 757–824.
48 K. Soai, T. Kawasaki and A. Matsumoto, *Acc. Chem. Res.*, 2014, **47**, 3643–3654.
49 K. L. Orchard, M. S. P. Shaffer and C. K. Williams, *Chem. Mater.*, 2012, **24**, 2443–2448.
50 J. Lewiński, W. Marciniak, Z. Ochal, J. Lipkowski and I. Justyniak, *Eur. J. Inorg. Chem.*, 2003, **43**, 2753–2755.
51 S. V. Athavale, A. Simon, K. N. Houk and S. E. Denmark, *Nat. Chem.*, 2020, **12**, 412–423.
52 M. Wolska-Pietkiewicz, A. Świerkosz, I. Justyniak, A. Grala, K. Sokołowski and J. Lewiński, *Dalton Trans.*, 2016, **45**, 18813–18816.
53 J. Lewiński, M. Dranka, W. Bury, W. Śliwiński, I. Justyniak and J. Lipkowski, *J. Am. Chem. Soc.*, 2007, **129**, 3096–3098.
54 *CrysAlisPro, Data Collection and Processing Software for Agilent X-ray Diffractometers*, ver. 1.171.35.21b, Agilent Technologies, 2012.
55 G. M. Sheldrick, *Acta Crystallogr., Sect. A: Found. Crystallogr.*, 2008, **64**, 112–122.
56 A. D. Becke, *J. Chem. Phys.*, 1993, **98**, 5648–5652.
57 C. Lee, W. Yang and R. G. Parr, *Phys. Rev. B: Condens. Matter Mater. Phys.*, 1988, **37**, 785–789.
58 S. Grimme, S. Ehrlich and L. Goerigk, *J. Comput. Chem.*, 2011, **32**, 1456–1465.
59 S. Grimme, J. Antony, S. Ehrlich and H. Krieg, *J. Chem. Phys.*, 2010, **132**, 15410.
60 K. Fukui, *Acc. Chem. Res.*, 1981, **14**, 363–368.
61 M. J. Frisch, G. W. Trucks, H. B. Schlegel, G. E. Scuseria, M. A. Robb, J. R. Cheeseman, G. Scalmani, V. Barone, G. A. Petersson, H. Nakatsuji, X. Li, M. Caricato, A. Marenich, J. Bloino, B. G. Janesko, R. Gomperts, B. Mennucci, H. P. Hratchian, J. V. Ortiz, A. F. Izmaylov, J. L. Sonnenberg, D. Williams-Young, F. Ding, F. Lipparini, F. Egidi, J. Goings, B. Peng, A. Petrone, T. Henderson, D. Ranasinghe, V. G. Zakrzewski, J. Gao, N. Rega, G. Zheng, W. Liang, M. Hada, M. Ehara, K. Toyota, R. Fukuda, J. Hasegawa, M. Ishida, T. Nakajima, Y. Honda, O. Kitao, H. Nakai, T. Vreven, K. Throssell, J. A. Montgomery Jr., J. E. Peralta, F. Ogliaro, M. Bearpark, J. J. Heyd, E. Brothers, K. N. Kudin, V. N. Staroverov, T. Keith, R. Kobayashi, J. Normand, K. Raghavachari, A. Rendell, J. C. Burant, S. S. Iyengar, J. Tomasi, M. Cossi, J. M. Millam, M. Klene, C. Adamo, R. Cammi, J. W. Ochterski, R. L. Martin, K. Morokuma, O. Farkas, J. B. Foresman and D. J. Fox, *Gaussian 16, Revision A.03*, Gaussian, Inc., Wallingford CT, 2016.
62 C. Y. Legault, *CYLview, 1.0b*, Université de Sherbrooke, 2009 (**https://www.cylview.org**).